0270-9139/88/0806-1521$02.00/0
HEPATOLOGY
Vol. 8, No. 6, pp. 1521–1529, 1988
Printed in U.S.A.

Heterogeneous Acinar Localization of the Asialoglycoprotein Internalization System in Rat Hepatocytes

PETER VAN DER SLUIJS†, INEKE BRAAKMAN, DIRK K. F. MEIJER AND GENY M. M. GROOTHUIS
Department of Pharmacology and Therapeutics, University of Groningen, Groningen, The Netherlands

Desialylated glycoprotein is rapidly cleared from plasma by a receptor-mediated endocytic mechanism located on hepatocytes. We studied the hepatic acinar distribution of this asialoglycoprotein transport system with the ligand ^{125}I-asialoorosomucoid using rat liver perfused in either antegrade or retrograde direction in combination with quantitative light microscopic autoradiography. Grain distribution along the acinus appeared dependent on the perfusion direction. A rather shallow zone 1 to zone 3 gradient was observed if livers were perfused in the normal direction. However, a statistically significantly steeper zone 3 to zone 1 gradient was detected in retrograde perfusions. Kinetic analysis of perfusate clearance profiles yielded a hepatic clearance of 21.6 ± 1.3 ml per min in antegradely perfused liver. Hepatic extraction was calculated to be 60.1 ± 7.4%. Biliary secretion of radioactivity amounted to 1.89 ± 0.18% of the dose within 1 hr after injection and consisted of intact material (1.39 ± 0.25%) and radioactive low-molecular-weight degradation products (0.52 ± 0.08%), of which more than 90% could be accounted for by ^{125}I$^-$. Apart from a minor difference regarding biliary secretion of an unidentified glycopeptide (less than 0.1% of the injected dose), transport data for the retrogradely perfused livers were identical to those obtained with livers perfused in antegrade direction, emphasizing the functional equivalence of both groups of livers. The autoradiographic data indicate that zone 3 hepatocytes take up ^{125}I-asialoorosomucoid more avidly than zone 1 cells. The kinetic and biochemical data indicate that further processing in the hepatocytes is virtually similar in the two zones. The functional significance of this higher uptake in zone 3 is presently unknown. A possible role in the mechanism of removal of senescent plasma proteins is discussed.

Received December 4, 1986; accepted March 31, 1988.

† Present address: European Molecular Biology Laboratory, Postfach 1022.09, 6900 Heidelberg, Federal Republic of Germany.

This study was supported by Grant 900-521-078 from the Netherlands' Foundation of Medical Research (MEDIGON), which is a subsidiary of the Netherlands' Organization for the Advancement of Pure Research (ZWO).

Portions of this work were presented at the 38th Annual Meeting of the American Association for the Study of Liver Diseases, Chicago, Illinois, in October, 1987, and were published in abstract form in Hepatology 1987; 7:1125.

Address reprint requests to: Geny Groothuis, Ph.D., Department of Pharmacology and Therapeutics, University of Groningen, Ant. Deusinglaan 2, NL-9713 AW Groningen, The Netherlands.

The involvement of a galactose-specific receptor on the rat hepatocyte plasma membrane in the endocytic removal of plasma asialoglycoproteins (ASGPs) is now well established [reviewed in Refs. (1–4)]. The hepatic uptake of ASGPs begins with binding of ligand to cell surface receptors and internalization via a coated pit-coated vesicle pathway (5). Shortly thereafter, ligand appears in smooth-membraned tubules and vesicles below the sinusoidal domain of the plasma membrane. After a series of vesicle fusions, ligand and receptor segregate, whereupon ligand is generally transported to lysosomes and receptor escapes immediate degradation by a recycling mechanism leading to reinsertion into the plasma membrane (6). A quantitatively minor number of vesicles escape from fusion with lysosomes and they discharge their contents at the canalicular membrane (7, 8). Elegant studies at the ultrastructural level elucidated the intracellular localization and internalization pathway of ligand and receptor (9–11). Surprisingly little, however, is known about the localization of the ASGP transport system in the different zones of the liver (12).

Sinusoidal blood flows from the terminal portal venule toward the terminal hepatic venule, causing different microenvironments around periportal (zone 1) and perivenous (zone 3) hepatocytes. A zonal heterogeneity is observed not only in ultrastructure, but also in metabolic (13, 14) and transport functions (15–17). In sinusoidal blood, a zone 1 to zone 3 concentration gradient of substances taken up efficiently by hepatocytes has been reported (16–18). Provided that hepatocytes along the acinus have equal transport characteristics, a similar concentration gradient would be anticipated inside the cells. Previously, St. Hilaire and associates (19) demonstrated such a gradient for the polypeptide epidermal growth factor. Presently, it is not clear whether this gradient is due to the different location of the cells regarding incoming blood, to intrinsic differences in uptake rate between the zones or to both. Transport experiments of Groothuis et al. (20) suggested a higher uptake rate in zone 1 of the ASGP dog intestinal alkaline phosphatase (21). These and other authors (20–22), however, also showed preferential binding of this ASGP to zone 3 hepatocytes in enzyme histochemical studies. Binding to this hepatocyte subpopulation could be inhibited completely by pretreatment of the rats with the selective

zone 3 toxin carbon tetrachloride (20), but hepatic uptake was not affected by this pretreatment.

In the immunocytochemical studies of Geuze et al. (9, 10) and in morphological studies of other groups (23–25), the acinar localization of the ASGP transport process was not addressed. We therefore investigated the localization of uptake of ^{125}I-ASOR in the various zones in antegradely and retrogradely perfused rat liver with quantitative light microscopic autoradiography and studied the further processing of the ASGP by kinetic and biochemical analyses of perfusate and bile in these perfusions.

MATERIALS AND METHODS

Animals. Male Wistar rats weighing 320 to 360 gm were from Harlan Sprague-Dawley Industries (Zeist, The Netherlands) and housed on woodchip bedding in Perspex cages in a temperature-controlled room with a 12-hr light/dark cycle. Animals were allowed free access to pelleted lab chow (Hope Farms, Woerden, The Netherlands) and water.

Chemicals. The following compounds were from the indicated sources: orosomucoid from the Netherlands' Red Cross, demineralized bovine serum albumin from Organon Teknika (Oss, The Netherlands), paraformaldehyde and glutaraldehyde from BDH (Amsterdam, The Netherlands), monoiodotyrosine (MIT) and diiodotyrosine (DIT) from Fluka (Buchs, Switzerland). All other reagents were from commercial sources described in recent reports from this laboratory (26–29).

Preparation of ^{125}I-Asialoorosomucoid (^{125}I-ASOR). Orosomucoid was nonenzymatically desialylated and radioiodinated to a specific activity of 2 to 8 μCi per μg (28, 29). Incorporation of the radiolabel was ascertained by sodium dodecyl sulfate-polyacrylamide gel electrophoresis (SDS-PAGE) and trichloroacetic acid (TCA) precipitation as described (28). ^{125}I-ASOR was stored at −30°C and used within 2 weeks after preparation. Immediately prior to all experiments, ^{125}I-ASOR was chromatographed on PD-10 columns. More than 99% of radioactivity in the void volume was precipitable with TCA at a final concentration of 10%.

Ex Vivo Perfused Rat Liver. The surgical techniques for antegrade and retrograde perfusions and the design of the perfused rat liver apparatus used in the studies reported herein have been described (15, 30). In short, fed male Wistar rats were anesthetized with pentobarbitone (Nembutal™, 60 mg per kg i.p.) and prepared for perfusion by cannulation of the common bile duct, portal vein and thoracic vena cava. Immediately after cannulation of the portal vein, *in situ* single-pass perfusion was initiated with Krebs bicarbonate buffer warmed to 38°C and oxygenated with 95% O_2/5% CO_2. The liver was excised and transferred to a thermostatically controlled cabinet. Perfusion was continued in the recirculating mode in either antegrade or retrograde direction with Krebs bicarbonate perfusate (100 ml), supplemented with 0.15 m*M* bovine serum albumin (1.0%) and 2 m*M* glucose. Flow of perfusate was adjusted to 2.5 to 3.5 ml per min per gm at a hydrostatic pressure of about 10 cm H_2O to ensure sufficient oxygen supply in the absence of erythrocytes. Temperature was kept at 38°C, and pH was measured on line and maintained between 7.35 and 7.44 either by slight adjustments in pCO_2 or by addition of a concentrated $NaHCO_3$ solution. Bile was collected in pretared polystyrene tubes and flow was determined gravimetrically assuming a density of 1 gm per ml.

Clearance and Biliary Excretion Studies. After a 20-min stabilization period, a tracer dose (80 pmoles) of ^{125}I-ASOR was rapidly injected into the mixing chamber of the perfusion apparatus, and the recirculating perfusion was continued for 60 min during which bile (10 min) fractions and perfusate were sampled. Samples were kept on ice; proteolytic products and protein-associated radioactivity were separated as described below. For biochemical characterization of radioactive (degradation) products, perfusate samples and pooled 30-min bile fractions were frozen and stored at −30°C until further analysis.

Analysis of Perfusate and Bile. Samples containing ^{125}I were assayed for protein-associated and TCA-soluble radioactivity. TCA was added to a final concentration of 10%. The precipitate was left to form on ice for 30 min and pelleted in an MSE Centaur benchtop centrifuge at 15,000 × g·min. The pellet was extracted with 20% TCA (final concentration) and after a further 30 min on ice, recentrifuged at 45,000 × g·min. Radioactivity in pellet and combined supernatants was counted as described (28).

Processing of Internalized Protein. Frozen bile samples were quickly thawed and diluted 2-fold with 1 m*M* potassium phosphate, 150 m*M* NaCl (pH 7.42), containing 0.1 m*M* phenylmethylsulfonyl fluoride. Insoluble material was removed by centrifugation at 100,000 × g·min in a microfuge. Clear supernatant was applied to a Sephadex G-25 fine column (45 x 0.90 cm) and eluted with 0.2 *M* acetic acid at a flow rate of 17 ml per hr; fractions of 3 ml were collected in tubes containing 1 ml of 1 *M* NaOH to prevent evaporative losses of $^{125}I_2$. The same protocol was utilized to analyze perfusate samples taken at 30 and 60 min after injection. In a separate run, the column was calibrated with a reference mixture containing unlabeled KI, MIT, DIT and ASOR; detection was as described (31), and the average recovery amounted to 100.5%. Bile samples were also analyzed by SDS-PAGE (32), with a 30:0.8 weight ratio of acrylamide to bisacrylamide. A 20-μl aliquot of bile was diluted with an equal volume of electrophoresis buffer (32) and subsequently denatured with β-mercaptoethanol for 5 min at 100°C. Samples were electrophoresed at 25 mA for 2 hr in the running gel. Gels were cut into 3-mm slices, and radioactivity in the slices was counted. To investigate whether the protein excreted into bile was unchanged ASOR, a pooled 60-min bile sample was made up to a final volume of 1 ml with phosphate-buffered saline and chromatographed on a PD-10 column with the same buffer. Radioactivity eluting at the void volume was pooled. More than 98% of this material could be precipitated with TCA. This was used for reinjection in a (second) isolated perfused liver. Reinjection studies were performed on the same day as the first experiment from which bile was isolated.

Quantitative Light Microscopic Autoradiography. Perfusate (100 ml) was recirculated through the liver in either antegrade or retrograde direction. At both 3 and 9 min after injection of 80 pmoles (15 μCi) ^{125}I-ASOR, intrahepatic distribution was assessed. At these timepoints, flow of perfusate was diverted and a 2-min wash (single pass) with ice-cold 20 m*M* sodium phosphate, 150 m*M* NaCl (pH 7.40) was started via an auxilliary input line. Livers were perfusion fixed (single pass) with the aforementioned buffer (0°C) containing 0.8% paraformaldehyde and 2.5% glutaraldehyde during a 4-min period. Immediately thereafter, portions of the major lobes were removed and cut into smaller blocks that were immersion fixed overnight with 2.5% glutaraldehyde in 20 m*M* sodium phosphate, 150 m*M* NaCl (pH 7.40). After dehydration and embedding, paraffin sections of 8 μm were mounted on coverslips and coated with Kodak NTB-3 nuclear emulsion. Following 3 to 6 wk exposure, slides were developed in Kodak D19 developer and stained with Grunwald Giemsa. Distribution of grains was quantitated using a Zeiss binocular light microscope at ×1,000 magnification, containing a calibrated reticule delineating 400 grid squares in one ocular. Each grid square encompassed an area of 25 μm^2. Only those grains that were located on hepa-

tocytes were counted. At each timepoint (3 and 9 min) 20 acini of duplicate livers were counted for both perfusion directions; the total number of acini assayed thus amounted to 80. The total number of grains counted for each perfusion direction was not significantly different.

Data Analysis. Half-life of liver uptake, $t_{1/2}$, was calculated from the initial slope of the semi-log perfusate concentration vs. time plot; uptake rate constant, $k = \ln(2)/t_{1/2}$; liver clearance, $Cl = 100 \times k$; extraction, $E = Cl/flow$. Biliary excretion vs. time plots were not corrected for intrahepatic and cannula transit time.

Grain distribution was calculated as follows: each acinus was divided into five parts. In each part the number of cross-sections in the grid coincident with a grain on a cell (A) and the number of cross-sections without a grain but on a cell (B) were counted. The percentage of grains in part i is then given by:

$$\frac{Ai/(Ai + Bi)}{\sum_{n=1}^{5} An/(An + Bn)} \cdot 100$$

Statistical comparisons were made with Student's t test after checking equality of variances with an F test (33), $p < 0.05$ was selected as the minimal level of statistical significance.

RESULTS

Kinetics and Extent of ASOR Uptake. Rat livers were perfused in the recirculating mode with a nonsaturating dose of 80 pmoles of ^{125}I-ASOR in antegrade or retrograde direction. Clearance curves of ^{125}I-ASOR are plotted in Figure 1. More than 98% was removed from perfusate within 15 min, irrespective of the perfusion direction. A semi-log plot of the perfusate concentration of precipitable radioactivity vs. time, as shown in the *insets*, reveals a straight line from which the hepatic uptake rate constants were calculated. Extraction efficiency of the uptake process was the same in both antegradely and retrogradely perfused livers. Kinetic parameters are given in Table 1. The data in Table 1 on bile and perfusate flow, portal vein pressure and liver weight show no statistically significant difference between antegrade and retrograde perfusion and indicate a similar viability in these groups of livers. Because livers were perfused in the absence of exogenously added bile salt, basal bile flow is somewhat low and approaches bile salt independent flow.

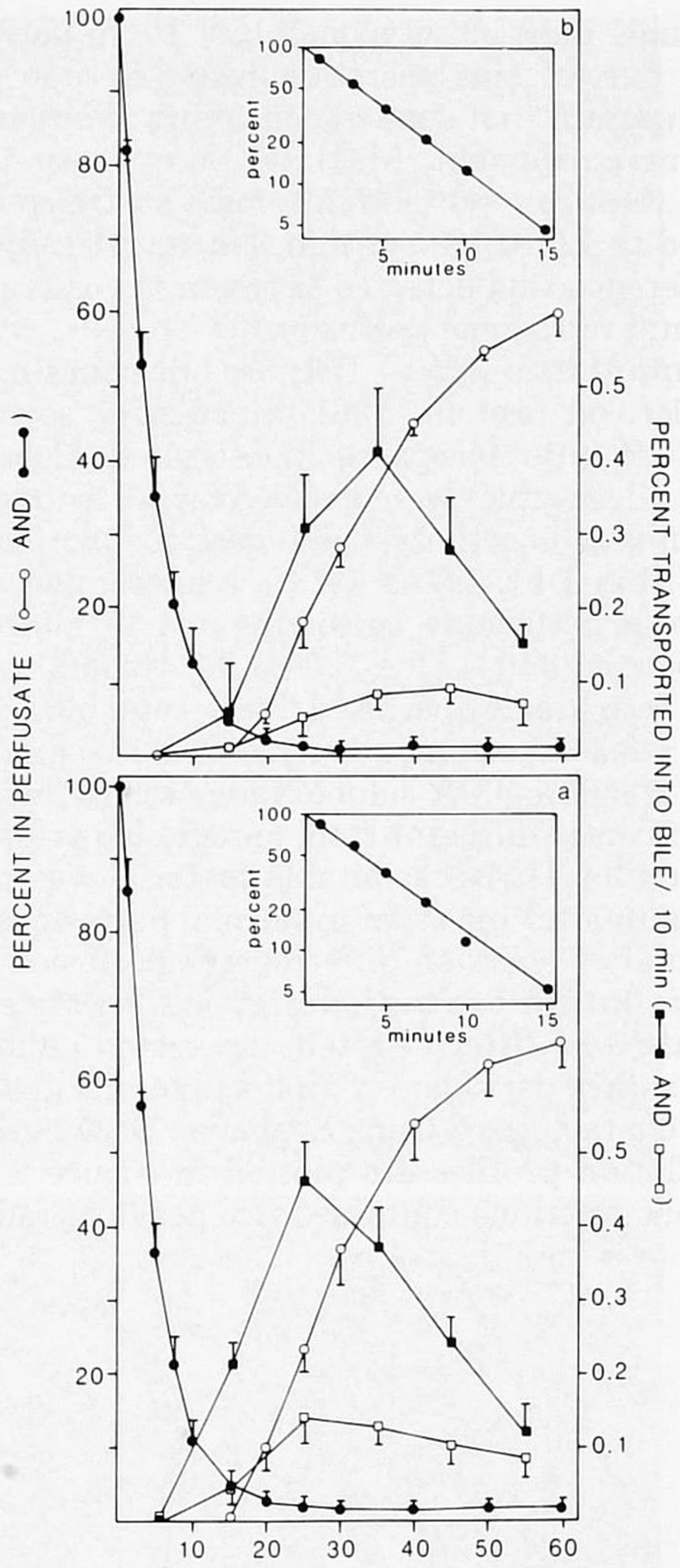

FIG. 1. Kinetics of ^{125}I-ASOR transport in antegradely (a) and retrogradely (b) perfused liver at 37°C. At the indicated times after injection of ^{125}I-ASOR, aliquots of perfusate (*circles*) were removed and precipitated with TCA. Radioactivity secreted into bile was determined in sequential 10-min fractions and plotted at the midcollection point (*squares*). Semi-log plots of precipitable radioactivity in perfusate during the first 15 min of perfusion are depicted in the *insets*. *Open symbols* = acid-soluble radioactivity; *closed symbols* = protein-associated radioactivity. Points = means ± S.D. of four or more experiments.

TABLE 1. Characteristics of perfused liver and ^{125}I-ASOR transport

	Antegrade	Retrograde
Portal vein pressure (cm H_2O)	10.6 ± 0.8	11.0 ± 0.9
Liver wt/body wt (%)	3.80 ± 0.27	3.80 ± 0.50
Bile flow/liver wt (μl/min/gm)	0.84 ± 0.16	0.69 ± 0.13
Perfusion flow/liver wt (ml/min/gm)	2.74 ± 0.19	2.49 ± 0.13
Hepatic uptake rate constant (per min)	0.204 ± 0.028	0.211 ± 0.039
Half-life in perfusate (min)	3.41 ± 0.51	3.33 ± 0.57
Perfusate flow (ml/min)	33.7 ± 1.3	32.2 ± 4.2
Clearance (ml/min)	21.6 ± 1.3	21.3 ± 3.7
Extraction efficiency (%)	60.1 ± 7.4	65.9 ± 7.5

Data are means ± S.D. of four experiments.

Secretion of Radioactive Degradation Products in Perfusate. TCA-soluble radioactivity appeared in perfusate 15 min postinjection in both antegradely and retrogradely perfused livers and release was sigmoidal as demonstrated in Figure 1. At 60 min after injection, about 65% of the injected dose was recovered in the perfusate as TCA-soluble radioactivity; this was increased to 87% after 2 hr of perfusion (not shown). Because it was reported previously that degradation products formed after addition of ^{125}I-ASOR (34) or ^{125}I-asialofetuin (35) to isolated perfused rat livers do not accumulate in the liver tissue, an estimate of the rate of hydrolysis of ASOR can be made from the appearance of

TCA-soluble radioactivity (mainly $^{125}I^-$) in perfusate. A semi-log plot of this secretion rate vs. time yields a biphasic pattern (not shown) consisting of a rising and a descending component. Maximal rate of secretion was achieved between 20 and 30 min postinjection and amounted to 2.5 to 3% per min. No statistically significant difference was detected between the curves of antegrade and retrograde perfusion.

Transport into Bile. Because bile contains several plasma-derived proteins (36), kinetics of secretion of radioactivity into bile were investigated. Sequentially collected bile samples were assayed for TCA-precipitable and -soluble radioactivity; these data are plotted in Figure 1. Within 1 hr, 1.89 ± 0.18% was secreted into bile in antegrade perfusions, consisting of 1.39 ± 0.25% protein-associated and 0.51 ± 0.08% TCA-soluble radioactivity. In retrogradely perfused livers, total biliary output was 1.58 ± 0.33%, composed of 1.28 ± 0.35% precipitable and 0.30 ± 0.08% TCA-soluble radioactivity, which was not significantly different from antegrade perfusion. Secretion rate of TCA-precipitable material was maximal 20 to 30 min after injection in normal perfusions and 30 to 40 min after injection in retrograde perfusion.

Fractionation of Radioactivity Recovered from Perfusate and Bile. Protein-associated radioactivity and radioactive degradation products in bile and perfusate were characterized using Sephadex G-25 chromatography. Elution profiles are plotted in Figure 2. Pooled 30-min bile fractions contained two peaks of radioactivity (*dashed lines*) corresponding with ^{125}I-ASOR and $^{125}I^-$. In normal perfusions, however, an extra (glyco)peptide eluting at 35 ml is apparent from Figure 2a. This unidentified peak contained 9.2% of the radioactivity applied on the column, which corresponds with 0.08% of the injected dose. Perfusate samples drawn at 30 and 60 min postinjection contained four radioactive species (Fig. 2, a to d, *solid lines*). Three components retained by the column were identified as $^{125}I^-$, [^{125}I]MIT and [^{125}I]DIT. The fourth component coeluted with unlabeled ASOR. The amounts of [^{125}I]MIT and [^{125}I]DIT secreted into perfusate were very low compared with the main metabolite $^{125}I^-$. At 30 min postinjection, 91.2% of TCA-soluble radioactivity was $^{125}I^-$, 8.32% was [^{125}I]MIT, whereas [^{125}I]DIT made up the remaining 0.45%. Corresponding figures for retrogradely perfused livers were: 89.7% $^{125}I^-$, 9.51% [^{125}I]MIT and 0.65% [^{125}I]DIT. At the end of the experimental period, [^{125}I]MIT and [^{125}I]DIT were quantitatively removed by the liver and deiodinated; no significant amounts of these compounds could be recovered at 60 min in both groups (Fig. 2, c and d).

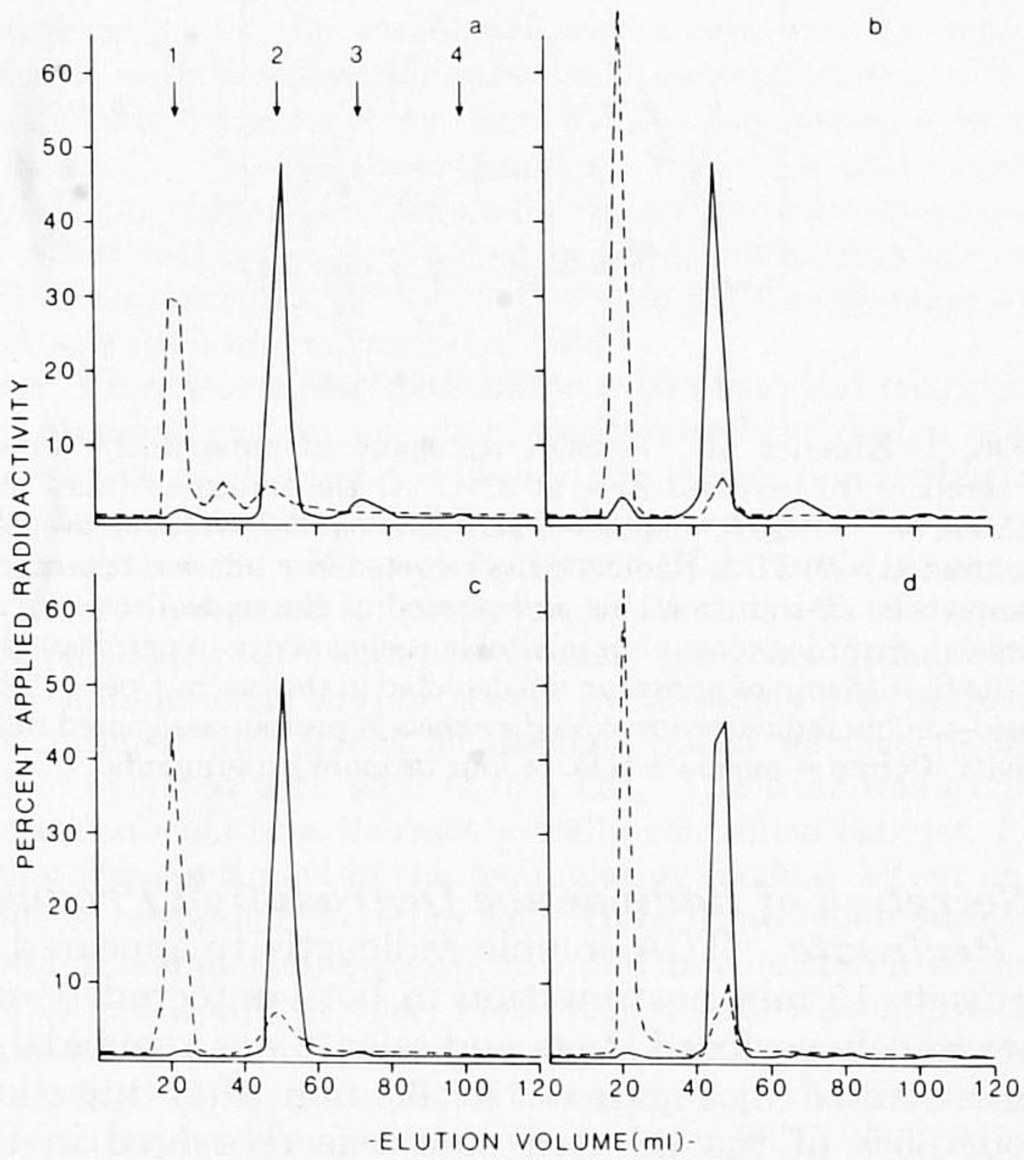

FIG. 2. Characterization of radioactivity in perfusate (*solid lines*) and bile (*dashed lines*) by gel filtration analysis on a Sephadex G-25 fine column (0.9 x 45 cm) in 0.2 *M* acetic acid. (a) Elution profiles of bile collected between 0 and 30 min and perfusate sampled at 30 min. (c) Bile collected between 30 and 60 min and perfusate sampled at 60 min. (b and d) Corresponding data on material obtained from retrogradely perfused livers. *Arrows* in (a) = elution positions of unlabeled references: ASOR (1), I^- (2), MIT (3) and DIT (4).

Characterization of Labeled Protein Recovered in Bile. Although a substantial amount, 73.5 to 81.0%, of radioactivity secreted into bile was TCA precipitable, this does not necessarily indicate that it is intact ^{125}I-ASOR. To characterize further the protein secreted into bile, bile fractions were analyzed by SDS-PAGE under reducing conditions. After counting radioactivity in 3-mm gel slices, more than 90% of the protein-associated radioactivity was recovered in the region of the 40 kD marker (ASOR).

To study whether the secreted protein was unchanged ASOR, we isolated this protein from bile and reinjected it into a second liver perfusion. The bile-derived radioactivity was cleared by this second liver with a half-life of 3.6 min in antegradely perfused liver and 3.4 min in a retrograde perfusion. These kinetic parameters are the same as those of the initially injected ^{125}I-ASOR (Table 1).

Quantitative Light Microscopic Autoradiography. At 3 or 9 min following injection of ^{125}I-ASOR, approximately 45 and 93% of the dose, respectively, was cleared from the perfusate. At these early timepoints, formation of (radioactive) degradation products is essentially negligible (Fig. 1), and the low-temperature wash and perfusion fixation protocol inhibit all intracellular endocytic events including degradation (37). Thus, radioactivity in the liver is only associated with ASOR. Localization of the injected ^{125}I-ASOR within the liver was visualized by light microscopic autoradiography and is shown in Figure 3. At 3 min postinjection, autoradiographic grains were almost exclusively colocalized with hepatocytes. Although it is difficult at the light microscopic level to document uptake by hepatocytes only, colocalization of grains with endothelial cells and Kupffer cells yields a very different pattern (38). Localization of silver grains was not uniform along the acinus. A gradient was observed descending from zone 1 to zone 3 cells upon perfusion in the normal direction (Fig. 3a).

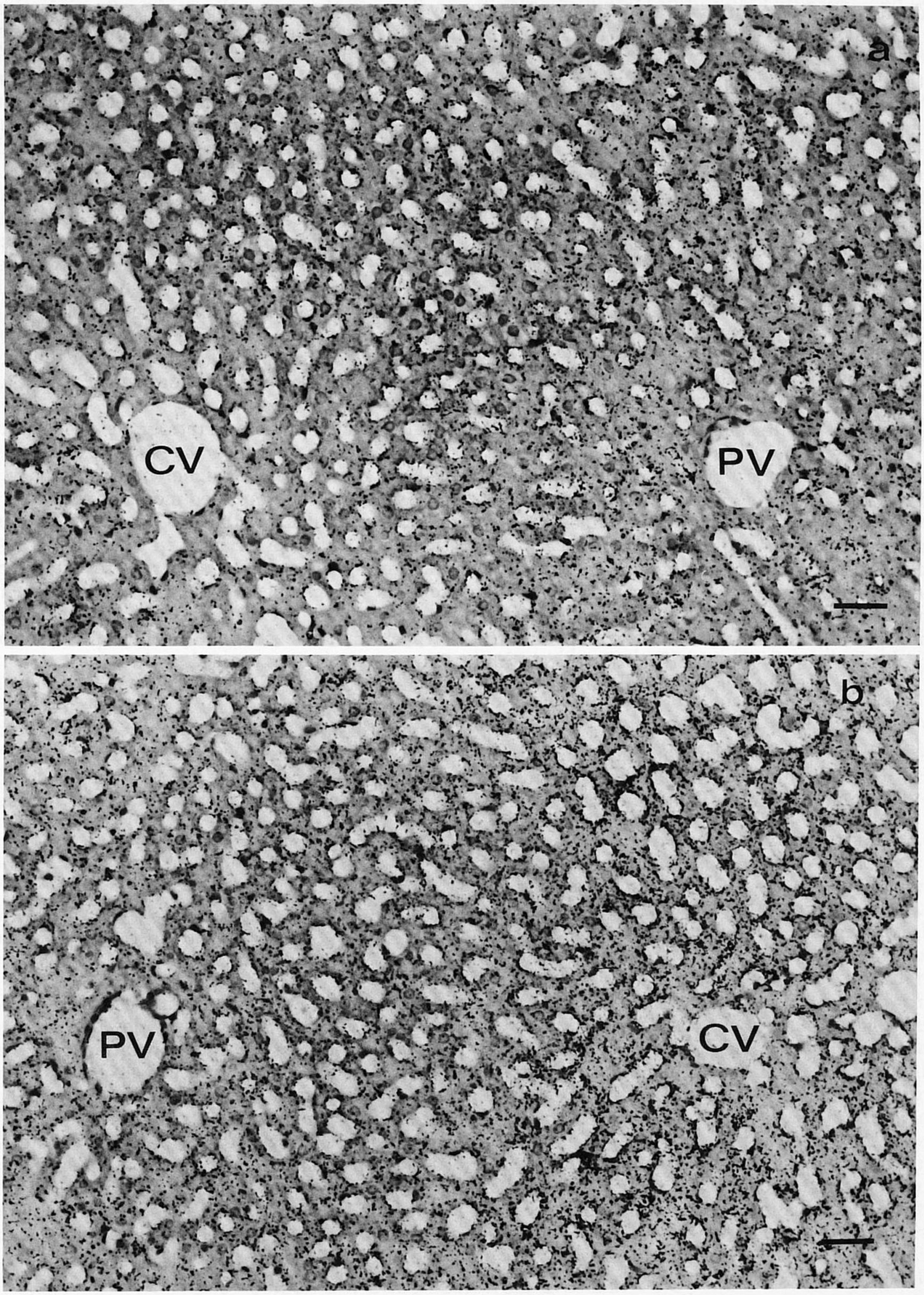

FIG. 3. Light microscopic autoradiographs of rat liver 3 min after injection of 80 pmoles (15 μCi) ^{125}I-ASOR, during antegrade (a) or retrograde (b) perfusion. Silver grains are found predominantly overlying hepatocytes. PV = portal venule; CV = central venule; *bar* = 28.5 μm. × 350.

This gradient was reversed if livers were perfused from zone 3 to zone 1 cells in the retrograde direction (Fig. 3b). At 9 min after injection of ^{125}I-ASOR, when uptake was practically complete, qualitatively similar grain distributions were observed when compared to the distributions obtained at 3 min after injection (not shown). Qualitative evaluation of these grain density distributions suggested a steeper gradient in grain density in the retrogradely perfused livers than in livers perfused in the normal direction.

Grains were counted in order to make a statistical evaluation of the grain densities in the different parts of the acinus. To calculate the grain distribution, we normalized the data, taking the number of grains in one acinus as 100%. This approach is more accurate than calculating the absolute number of counted grains, because a correction is made for the variety in tissue architecture per acinus (e.g. the length of the acinus and the space occupied by sinusoids). The data are shown in Figure 4. To test whether the zone 3 to zone 1 gradients were steeper than the zone 1 to 3 gradients, the mirror images of the zone 3 to zone 1 gradients were constructed with a perpendicular line through the midpoint of the acinus as the mirror axis (Fig. 4, *dashed curves*). The data of corresponding points in the curves from antegrade and retrograde perfusions were compared. Statistical comparison of these data pairs at a given relative acinar distance unambiguously demonstrated that the zone 3 to zone 1 gradient was significantly steeper than the zone 1 to zone 3 gradient at both timepoints.

DISCUSSION

In this study, we investigated whether transport and processing of ASOR is heterogeneously distributed over the hepatocytes of the acinus. This issue was addressed by quantitative autoradiography after injection of ^{125}I-ASOR in rat liver, perfused in antegrade or retrograde direction, in combination with kinetic and biochemical experiments. The results of the quantitative autoradiography (Fig. 4) show a gradient decreasing from zone 1 to zone 3 after administration of ASOR in an antegrade perfusion and a much steeper and reversed gradient in a retrograde perfusion. These results indicate a higher uptake activity in zone 3 cells compared to zone 1 cells. This is concluded from the following considerations: if all cells had the same uptake activity, the concentration gradient in the cells along the acinus should be parallel to the concentration gradient in the sinusoids, as was originally proposed by Goresky et al. (18). In addition, the tissue gradient in retrograde perfusion should then be the exact mirror image of the one obtained after antegrade perfusion, as was previously found for rhodamine B (39).

The steeper gradient in retrograde perfusion compared to antegrade perfusion can be readily explained when the cells in zone 3 have a higher uptake activity than the cells in zone 1. A simplified model as shown in Figure 5, a and b, can illustrate this observation. The figure shows that if the uptake activity in zone 3, defined as the fraction of the amount in perfusate extracted by this zone, is for instance 1.67 times higher than in zone 1, the tissue gradient of the retrograde perfusion is much steeper than one obtained during antegrade perfusion. This steepness is expressed as the zone 1 to zone 3 ratio in antegrade perfusion and the zone 3 to zone 1 ratio in retrograde perfusion. The same figure also shows that, despite these differences in uptake activity in the zones of the acinus, the extraction ratio and thus the clearance are the same in antegrade and retrograde perfusion. This is independent of the magnitude of the uptake activity

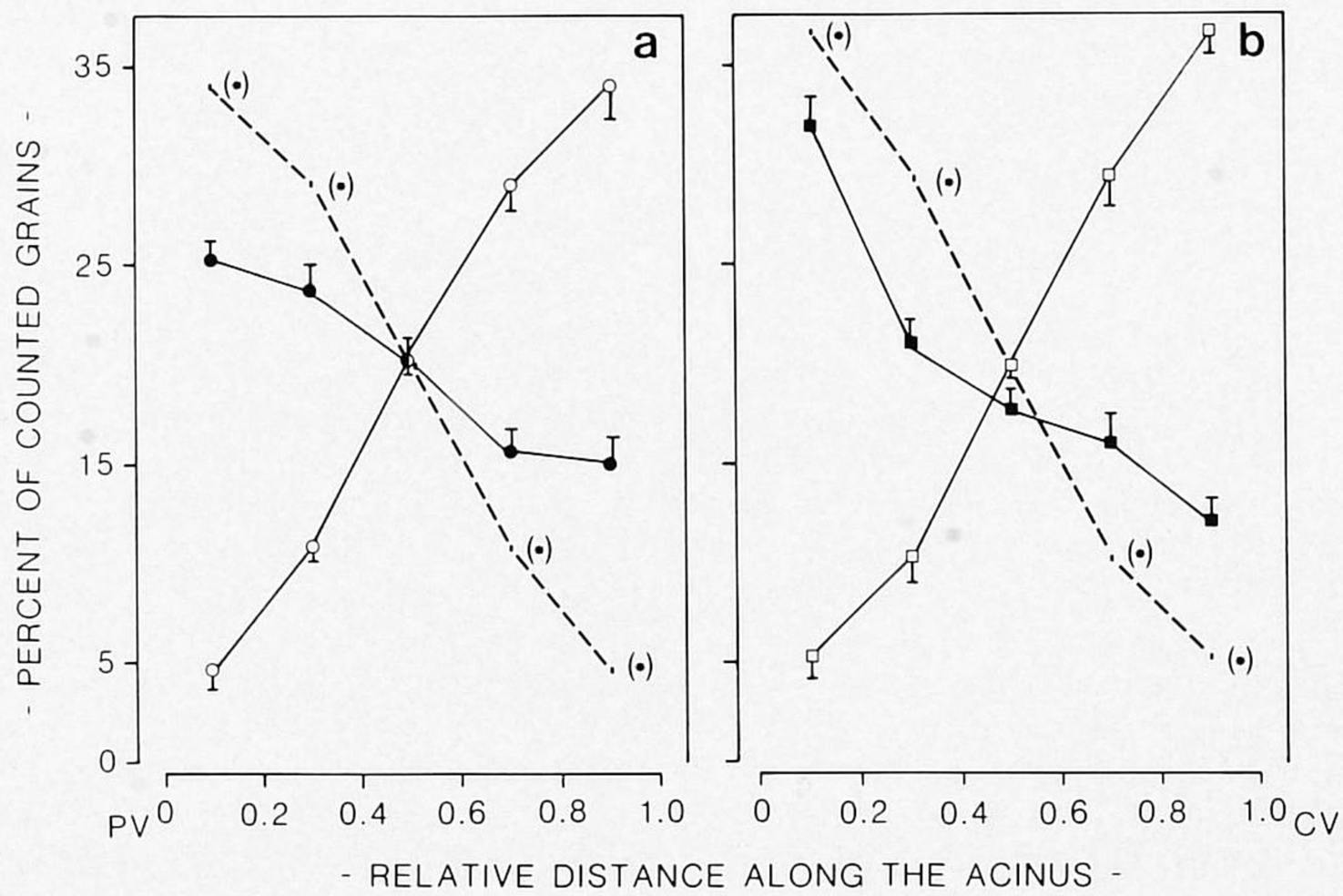

FIG. 4. Distribution of autoradiographic grains after injection of ^{125}I-ASOR at 3 (a) or 9 min (b) in normal (*closed symbols*) and retrograde perfusions (*open symbols*). The hepatic acinus was divided into five equally spaced sections, and grain distribution was assessed as described in "Materials and Methods." *Points* = means ± S.E. of 20 acini from two livers. *Asterisks* = statistical differences between the elements of corresponding data pairs ($p < 0.001$). PV = portal venule; CV = central venule. The mirror image of the zone 3 to zone 1 gradient is given by the *dashed profile*, half the acinus length being the mirror axis.

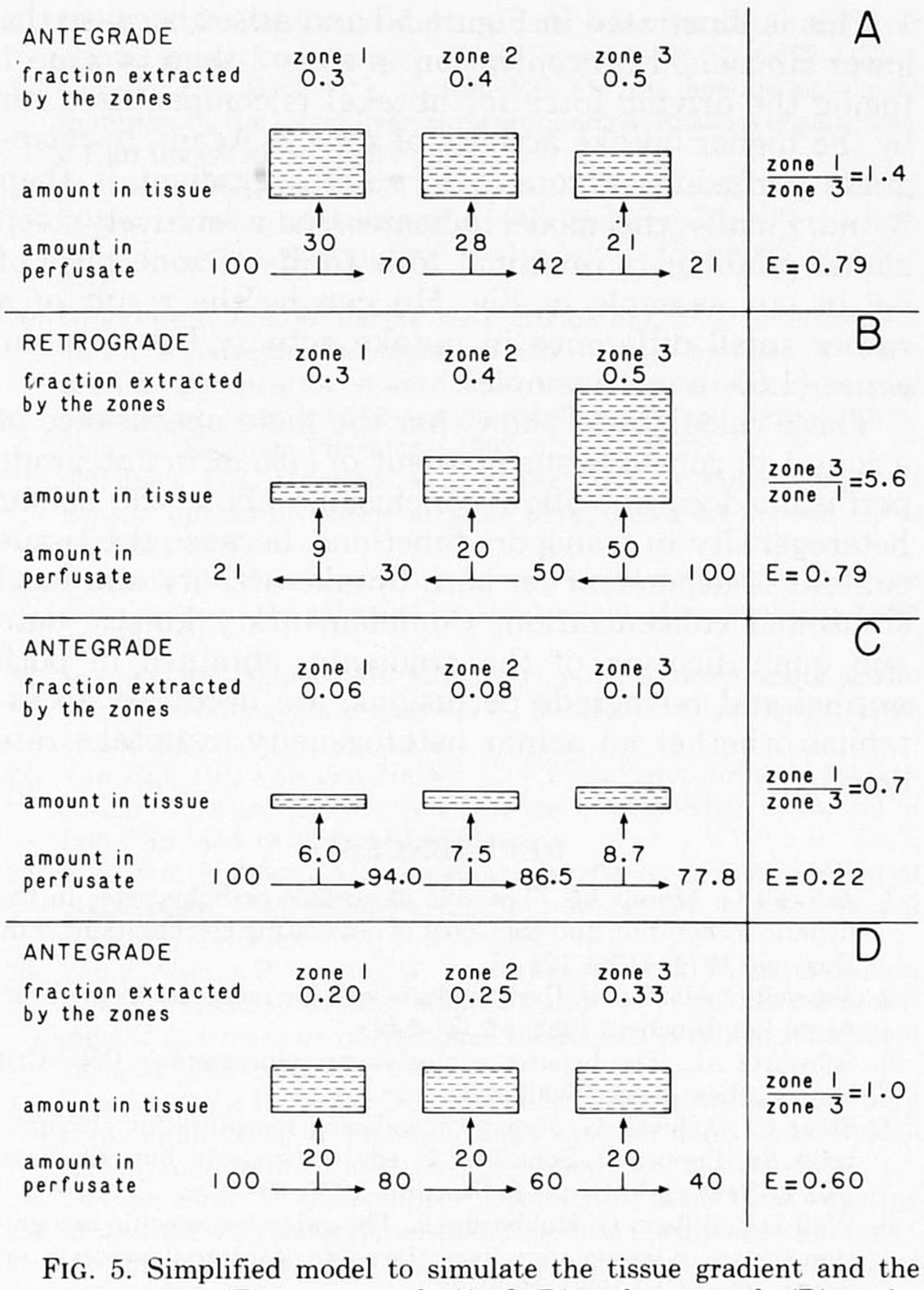

FIG. 5. Simplified model to simulate the tissue gradient and the extraction ratio (E) in antegrade (A, C, D) and retrograde (B) perfusions. (A and B) The extraction fractions of zones 1, 2 and 3 are arbitrarily set at 0.3, 0.4 and 0.5, respectively. The amount in tissue is indicated by the *hatched areas*, and the tissue gradient is expressed as amount in zone 1/amount in zone 3 in antegrade perfusion, and as amount in zone 3/amount in zone 1 in retrograde perfusion. The extraction ratio of the whole liver is 0.79 in both perfusions. (C) At low hepatic extraction ratio, a higher extraction fraction in zone 3 results in a tissue gradient increasing from zone 1 to zone 3 in antegrade perfusion. (D) The tissue distribution can be homogeneous, despite a different extraction fraction in the three zones.

and the number of sequential compartments (not shown). This was confirmed with computer simulation (40). (In Appendix I the consequences of these considerations are worked out in more detail.) Thus, the similarity of the initial phases of the plasma disappearance curves are fully compatible with the observed gradients and should be regarded as another indication of similar viability of the livers perfused in normal and retrograde direction.

From Figure 4 it can be calculated that in antegrade perfusion about 60% of the dose is taken up and processed in zone 1 cells, whereas in retrograde perfusion this amounts to only 15%. Consequently, zonal differences in secretion and/or metabolic rates should in principle lead to differences in rate of metabolism and excretion. Our data on degradation and secretion, however, do not show significant differences between antegrade and retrograde perfusion. Only two slight differences were found. First, the maximal biliary excretion rate is reached in the 20- to 30-min interval in normal perfusions and in the 30- to 40-min interval in the retrograde perfusions. This can be explained at least in part by the longer bile cannula used in retrograde perfusions, leading to an approximately 4-min longer lag-time in the biliary secretion curve compared to antegrade perfusions. Second, the appearance of the small (glyco)peptide peak in gel filtration (Fig. 2). This fraction contained only 0.08% of the injected dose and is therefore of minor importance. Accordingly, we conclude that all cells in the acinus have the same metabolic and excretion rate for ^{125}I-ASOR and its metabolites.

The quantitative data on the higher uptake rate of ASOR in zone 3 are in line with the histochemical results obtained with the ASGP dog intestinal alkaline phosphatase (20, 22): this protein showed higher binding to zone 3 cells. The conclusions based on the enzyme histochemical methods used in those studies, however, rely on the assumption that no enzyme activity is lost due to binding to zone 1 cells. A zone 1 to zone 3 gradient was also observed for epidermal growth factor (41, 42), but no data on this polypeptide are available from retrograde perfusions. In autoradiographic studies with other plasma-borne proteins like insulin (43), immunoglobulin A (44) and apoprotein B (45), no acinar gradient was reported.

Several mechanisms may underlie the observed heterogeneity in uptake rate of ASOR, such as differences in sinusoidal anatomy or intrinsic cellular differences. It is not very likely that zonal differences in fenestrae diameter (46) lead to a higher uptake rate in zone 1, because the Stokes radius of a 40 kD glycoprotein is about 7.5 nm (47–49), being less than 5% of the average fenestrae diameter (46). In addition, there are indications that the 30% higher porosity of the sinusoidal lining in zone 3 in comparison with zone 1 (50) has no influence on the uptake rate in the zones (39). However, the greater tortuosity and higher surface to volume ratio of the sinusoids in the periportal area (51) should have favored the uptake rate in zone 1, and the intrinsic difference in endocytic activity might even be underscored. Intrinsic differences between the cells regarding the number of receptors could well be the reason for the differences in uptake rate, as is also suggested for dog intestinal alkaline phosphatase (20, 22). This could perhaps be studied with (immunogold) cytochemistry (9), but this technique demonstrates antigenically active receptors, which need not all be functionally active in the endocytic process.

Uptake experiments with isolated hepatocytes, separated into fractions enriched in zone 1 or zone 3 cells, would provide an answer to the question concerning intrinsic differences. Up to now, the separation techniques available do not result in sufficient purity of the fractions or rely on the presence of the membrane perturbant digitonin during the isolation procedure (52, 53), which may disturb cellular transport functions. Perfused rat liver currently is the best preparation available to investigate hepatocyte heterogeneity in transport functions (54). *In vitro* binding of ASOR to membranes obtained from whole liver homogenates revealed only one class of binding sites (1). This renders the concept

of different affinities of the receptor in zone 1 and zone 3 less likely.

The physiological significance of a more avid uptake process in zone 3 cells remains to be established, the more so since the role of the receptor awaits characterization. In view of recent findings on ceruloplasmin transport (55, 56), it could be speculated that zone 3 hepatocytes form the terminal branch of a removal system for senescent plasma glycoproteins desialylated by endothelial cells. After being released as ASGP in the sinusoids/Disse space, they might interact with the ASGP receptor and subsequently be internalized and degraded in hepatocytes. A more active internalization system at the end of the acinus could minimize spillover of these immunogens in the general circulation.

Acknowledgments: We thank Dr. P. Nieuwenhuis (Department of Histology, University of Groningen) for making his laboratory available to us; J. Bun (Department of Histology, University of Groningen) for performing autoradiography; Dr. J. Koudstaal for his help with the morphometric analysis; R. Oosting for technical assistance; A. M. M. Ellison for word-processing, and Dr. H. J. Geuze for helpful suggestions.

APPENDIX I

This appendix contains an analysis of the interpretation of observed gradients using a simplified model in which the liver is divided into 3 zones. The uptake activity of each zone is expressed as the fraction of the amount in perfusate that is extracted in this zone. Such model calculations might be very helpful to understand the impact of acinar heterogeneity in transport functions on the tissue distribution of a substrate. The following calculations are based on the assumption of first-order transport kinetics in all zones.

If zone 3 has a higher uptake activity than zone 1, at first sight a higher tissue concentration in zone 3 than in zone 1 would be expected. Figure 5a clearly shows, however, that when the total hepatic extraction is quite high, 0.79 in our example, the tissue concentration in zone 1 can be higher than in zone 3, despite a higher uptake activity in zone 3 than in zone 1. This can be accounted for by the rather high amount of substrate taken up in zone 1 and zone 2. The sinusoidal concentration presented in zone 3 is so much lower than in zone 1 (42 and 100 arbitrary units, respectively, in our example) that the tissue content (as a product of the fraction extracted and sinusoidal substrate concentration) is lower in zone 3 than in zone 1. A relatively higher amount in zone 3 can only be achieved when the total hepatic extraction is quite low. This is illustrated in Figure 5c, where the extraction (E) by the liver is only 0.22. Again (as in Fig. 5a), the uptake activity in zone 3 is 1.67 times higher than in zone 1. In this case, the amount taken up in zone 3 is higher than in zone 1, and a zone 1 to zone 3 ratio of 0.69 is found. In all such cases, a retrograde perfusion should show a steeper gradient decreasing from zone 3 to zone 1 (see Fig. 5b). In addition, it should be realized that a homogeneous acinar distribution found for a substrate with a relatively high extraction ratio implies a higher uptake activity in zone 3 than in zone 1. This is illustrated in Figure 5d and arises because the lower sinusoidal concentration in zone 3 than in zone 1 (being the driving force for uptake) is compensated for by the higher uptake activity of zone 3. Again, in retrograde perfusions a zone 3 to zone 1 gradient is then found. Finally, this model indicates that a relatively steep acinar gradient (a proximal zone to distal zone ratio of 5.6 in our example in Fig. 5b) can be the result of a rather small difference in uptake activity between the zones (1.67 in our example).

These calculations show that the mere appearance of a zone 1 to zone 3 tissue gradient *in vivo* or in antegrade perfusion does not allow conclusions about the acinar heterogeneity in transport functions, because the tissue content is dependent on both uptake activity and local sinusoidal concentration. Complementary kinetic data and quantification of the gradients, obtained in both normal and retrograde perfusions, are necessary to establish whether an acinar heterogeneity in uptake rate does exist.

REFERENCES

1. Ashwell G, Morell AG. The role of surface carbohydrates in the hepatic recognition and transport of circulating glycoproteins. Adv Enzymol 1974; 41:99–128.
2. Ashwell G, Harford J. Carbohydrate specific receptors in the liver. Annu Rev Biochem 1982; 51:531–544.
3. Schwartz AL. The hepatic asialoglycoprotein receptor. CRC Crit Rev Biochem 1984; 16:207–223.
4. Steer CJ, Ashwell G. Hepatic membrane receptors for glycoproteins. In: Popper H, Schaffner F, eds. Progress in liver diseases, Vol. 8. New York: Grune & Stratton. 1986; 99–123.
5. Wall DA, Wilson G, Hubbard AL. The galactose specific recognition system of mammalian liver: the route of internalization in rat hepatocytes. Cell 1980; 21:79–93.
6. Bridges K, Harford J, Ashwell G. Fate of receptor and ligand during endocytosis of asialoglycoproteins by isolated hepatocytes. Proc Natl Acad Sci USA 1982; 79:350–354.
7. Schiff JM, Fischer MM, Underdown BJ. Receptor mediated biliary transport of immunoglobulin A and asialoglycoprotein: sorting and missorting of ligands revealed by two radiolabeling methods. J Cell Biol 1984; 98:79–88.
8. Schiff JM, Fischer MM, Jones AL, et al. Human IgA as a heterovalent ligand switching from the asialoglycoprotein receptor to secretory component during transport across the hepatocyte. J Cell Biol 1986; 102:920–931.
9. Geuze HJ, Slot JW, Strous GJAM, et al. Immunocytochemical localization of the receptor for asialoglycoprotein in rat liver cells. J Cell Biol 1982; 92:865–870.
10. Geuze HJ, Slot JW, Strous GJAM, et al. Intracellular site of asialoglycoprotein receptor ligand uncoupling: double label immunoelectronmicroscopy during receptor mediated endocytosis. Cell 1983; 32:277–287.
11. Geuze HJ, Slot JW, Strous GJAM, et al. Intracellular receptor sorting during endocytosis: comparative immunoelectronmicroscopy of multiple receptors in rat liver. Cell 1984; 37:195–204.
12. Rappaport AM, Borowy ZJ, Lougheed WM, et al. Subdivision of hexagonal liver lobules into a structural and functional unit. Role in hepatic physiology. Anat Rec 1954; 119:11–27.
13. Jungerman K, Katz N. Functional hepatocellular heterogeneity. Hepatology 1982; 2:385–395.
14. Thurman RG, Kauffman FC. Sublobular compartmentation of pharmacologic events (SCOPE): metabolic fluxes in periportal and pericentral regions of the liver lobule. Hepatology 1985; 5:144–151.
15. Groothuis GMM, Hardonk MJ, Keulemans KPT, et al. Autoradiographic and kinetic demonstration of acinar heterogeneity of taurocholate transport. Am J Physiol 1982; 243:G455–G462.
16. Groothuis GMM, Hardonk MJ, Meijer DKF. Hepatobiliary transport of drugs: do periportal and perivenous hepatocytes perform the same job? Trends Pharmacol Sci 1985; 6:322–327.

17. Gumucio JJ. Functional and anatomic heterogeneity in the liver acinus: impact on transport. Am J Physiol 1983; 244:G578–G582.
18. Goresky CA, Bach GG, Nadeau BE. On the hepatic uptake of materials by the intact liver: transport and net removal of galactose. J Clin Invest 1973; 52:991–1009.
19. St. Hilaire RJ, Hradek GT, Jones AL. Hepatic sequestration and biliary secretion of epidermal growth factor: evidence for a high capacity uptake system. Proc Natl Acad Sci USA 1983; 80:3797–3801.
20. Groothuis GMM, Weitering JG, Hardonk MJ, et al. Heterogeneity of rat hepatocytes in transport and hepatic binding of asialo alkaline phosphatase studied after induction of selective acinar damage by N-hydroxy-2-acetylaminofluorene and carbon tetrachloride. Biochem Pharmacol 1983; 32:2721–2727.
21. Scholtens HB, Hardonk MJ, Meijer DKF. A kinetic study of hepatic uptake of canine alkaline phosphatase in the rat. Liver 1982; 2:1–13.
22. Hardonk MJ, Scholtens HB. A histochemical study about the zonal distribution of the galactose binding protein. Histochemistry 1980; 69:289–297.
23. Stockert RJ, Haimes HB, Morell AG, et al. Endocytosis of asialoglycoprotein enzyme conjugates by hepatocytes. Lab Invest 1980; 43:556–563.
24. Van Rijk PP, Van den Hamer C. ^{131}I-asialoglycoprotein. Investigation of its use for liver function tests; metabolism in the rat. J Lab Clin Med 1976; 88:142–150.
25. Wall DA, Hubbard AL. Galactose specific recognition system of mammalian liver: receptor distribution on the hepatocyte cell surface. J Cell Biol 1981; 90:687–696.
26. Van der Sluijs P, Oosting R, Weitering JG, et al. Biliary secretion of FITC metabolites after administration of FITC-labeled orosomucoid as a measure of lysosomal hydrolysis. Biochem Pharmacol 1985; 34:1399–1405.
27. Van der Sluijs P, Meijer DKF. Binding of drugs with a quaternary ammonium group to alpha$_1$-acid glycoprotein and asialo alpha$_1$-acid glycoprotein. J Pharmacol Exp Ther 1985; 234:703–707.
28. Van der Sluijs P, Bootsma HP, Postema B, et al. Drug targeting to the liver with lactosylated albumins: does the glycoprotein target the drug or is the drug targeting the glycoprotein? Hepatology 1986; 6:723–728.
29. Van der Sluijs P, Spanjer HH, Meijer DKF. Hepatic disposition of cationic drugs bound to orosomucoid: lack of coendocytosis and evidence for intrahepatic dissociation. J Pharmacol Exp Ther 1987; 240:668–673.
30. Meijer DKF, Keulemans K, Mulder GJ. Isolated perfused rat liver technique. Methods Enzymol 1981; 77:81–94,
31. LaBadie JH, Chapman KP, Aronson NN Jr. Glycoprotein catabolism in rat liver. Lysosomal degradation of iodinated asialofetuin. Biochem J 1975; 77:271–279.
32. Laemmli UK. Cleavage of structural proteins during the assembly of the head of bacteriophage T4. Nature 1970; 227:680–685.
33. Snedecor GW, Cochran WG. Statistical methods, Ed. 7. Ames, Iowa: Iowa State University Press, 1980.
34. Dennis PA, Aronson NN Jr. Uptake and degradation of ^{125}I-labeled rat asialoorosomucoid by the perfused rat liver. Biochim Biophys Acta 1983; 798:14–20.
35. Dunn WA, LaBadie JH, Aronson NN Jr. Inhibition of ^{125}I-asialofetuin catabolism by leupeptin in the perfused rat liver and *in vivo*. J Biol Chem 1979; 254:4191–4196.
36. Kloppel TM, Brown WR, Reichen J. Mechanisms of secretion of proteins into bile: studies in the perfused liver. Hepatology 1986; 6:587–594.
37. Dunn WA, Hubbard AL, Aronson NN Jr. Low temperature selectively inhibits fusion between pinocytic vesicles and lysosomes during heterophagy of ^{125}I-asialofetuin by the perfused rat liver. J Biol Chem 1980; 255:5971–5978.
38. Hubbard AL, Wilson G, Ashwell G, et al. An electron-microscope autoradiographic study of the carbohydrate recognition systems in rat liver. 1. Distribution of ^{125}I-ligands by the perfused rat liver. J Cell Biol 1979; 83:47–64.
39. Braakman I, Groothuis GMM, Meijer DKF. Acinar redistribution and heterogeneity in transport of the organic cation rhodamine B in rat liver. Hepatology 1987; 7:849–855.
40. Groothuis GMM, Keulemans KPT, Hardonk MJ, et al. Acinar heterogeneity in hepatic transport of dibromosulphthalein and ouabain studied by autoradiography, normal and retrograde perfusions and computer simulations. Biochem Pharmacol 1983; 32:3069–3078.
41. St. Hilaire RJ, Jones AL. Epidermal growth factor: its biological and metabolic effects with emphasis on the hepatocyte. Hepatology 1982; 2:601–613.
42. Chabot JG, Walker P, Pelletier G. Distribution of epidermal growth factor binding sites in the adult rat liver. Am J Physiol 1986; 250:G760–G764.
43. Renston RH, Maloney DG, Jones AL, et al. Bile secretion apparatus: evidence for a vesicular transport mechanism for proteins in the rat using horseradish peroxidase and ^{125}I-insulin. Gastroenterology 1980; 78:1373–1378.
44. Renston RH, Jones AL, Christiansen WD, et al. Evidence for a vesicular transport mechanism in hepatocytes for biliary secretion of immunoglobulin A. Science 1980; 208:1276–1278.
45. Chao YS, Jones AL, Hradek GT, et al. Autoradiographic localization of the sites of uptake, cellular transport, and catabolism of low density lipoproteins in liver of normal and estrogen treated rats. Proc Natl Acad Sci USA 1981; 78:597–601.
46. De Zanger R, Wisse E. The filtration effect of rat liver fenestrated sinusoidal endothelium on the passage of remnant chylomicrons to the space of Disse. In: Knook DL, Wisse E, eds. Sinusoidal liver cells. Amsterdam: Elsevier Biomedical Press, 1982: 69–76.
47. Cantor CR, Schimmel PR. Biophysical chemistry, part 2. Techniques for the study of biological structure and function. San Francisco: W. H. Freeman & Co., 1980: 539–685.
48. Montreuil J, Debray H, Debeire P, et al. Lectins as oligosaccharide receptors. In: Popper H, Reutter W, Gudat F, et al., eds. Structural carbohydrates in the liver. Boston: MTP Press, Ltd., 1983: 239–258.
49. Moore WJ. Physical chemistry, Ed. 5. London: Longman Group, Ltd., 1972: 945–946.
50. Wisse E, De Zanger RB, Jacobs R, et al. Scanning electron microscope observations on the structure of portal veins, sinusoids and central veins in rat liver. Scan Electron Microsc 1983; 3:1441–1452.
51. Miller DL, Zanolli CS, Gumucio JJ. Quantitative morphology of the sinusoids of the hepatic acinus. Gastroenterology 1979; 76:965–969.
52. Lindros KO, Pentilla KA. Digitonin-collagenase perfusion for efficient separation of periportal and perivenous hepatocytes. Biochem J 1985; 228:757–760.
53. Quistorff B. Glucogenesis in periportal and perivenous hepatocytes of rat liver by a new high-yield digitonin-collagenase perfusion technique. Biochem J 1985; 229:221–226.
54. Javitt NB. Hepatic heterogeneity: backward perfusion—a forward step. Lab Invest 1987; 56:565–567.
55. Tavassoli M, Kishimoto T, Katakoa M. Liver endothelium mediates the hepatocyte's uptake of ceruloplasmin. J Cell Biol 1986; 102:1298–1303.
56. Irie S, Tavassoli M. Liver endothelium desialylates ceruloplasmin. Biochem Biophys Res Commun 1986; 140:94–100.